Available online at www.sciencedirect.com

ScienceDirect

Procedia CIRP 103 (2021) 280–285

www.elsevier.com/locate/procedia

9th CIRP Global Web Conference – Sustainable, resilient, and agile manufacturing and service operations : Lessons from COVID-19

Design of a parallel robot with additively manufactured flexure hinges for a cryogenic work environment

Philipp Jahn[a]*, Frank Ihmig[b], Annika Raatz[a]

[a]*Leibniz University Hannover, Institute of Assembly Technology, An der Universität 2, 30823 Garbsen, Germany*
[b]*Fraunhofer Institute for Biomedical Engineering, Joseph-von-Fraunhofer-Weg 1, 66280 Sulzbach, Germany*

* Corresponding author. Tel.: +49-511-762-18250; fax: +49-511-762-18245. *E-mail address:* Jahn@match.uni-hannover.de

Abstract

Automation is ubiquitous in today's industrial landscape and is finding its way into more and more highly specialised applications - also in the field of cryopreservation. The extreme work conditions in cryobanks place exceptionally high demands on the mechanical and electronic components used. The preservation and storage of biological samples take place at temperatures between -130 °C and -196 °C using liquid nitrogen as a cooling medium. The bearings and joints used in industrial parallel kinematic robots (for example, ball bearings or Cardan joints) jam at these ambient parameters and are unsuitable for an application within a cryobank. We, therefore, develop methods and technologies to enable fully automated handling of biological samples under cryogenic working conditions. The basis for this is a parallel kinematic robot structure that allows the drives to be placed outside the cold environment. In contrast, the rest of the robot structure can be actuated in a cryogenic container.

In this context, the passive joints for this parallel robot are designed as additively manufactured monolithic flexure hinges. This paper presents the design, simulation, and construction of the parallel robot and focuses on the flexure hinges fabricated using the selective laser melting process (SLM). We describe the design of the flexure hinges, their intended use in the robot, and the experimental setup used for their validation. We also compare the operating parameters recorded in experiments (such as bending angle, bending moment) with the data obtained in finite element method simulations (FEM). In addition, we describe the geometric constraints and deviations of the manufactured joints due to the manufacturing process.

Keywords: flexure hinges; compliant mechanisms; cryobank; cryopreservation; parallel robots;

1. Introduction

In recent years, the demand for high-quality, long-term storage and preservation of organic cell material has increased considerably. Not least, the global pandemic of the SARS CoV-2 virus and the accompanying need for research has caused the number of cryobanks to grow rapidly [1]. However, existing cryobanks show significant differences both in terms of their technical equipment and in terms of their freezing and thawing procedures derived from their research as well as from practical experience.

In today's industry, automation is an omnipresent factor, even in niche applications such as cryopreservation. However, manual handling of biological or toxic samples is still the norm in research facilities. Sample containers are often moved in, out or around by hand using bulky protective clothing. These procedures present both a significant risk of injury to personnel from cold burns and a threat to sample integrity from damage.

10.1016/j.procir.2021.10.045

To overcome these challenges, full automation is required at temperatures below -130 °C [2].

Against the background of these problems, we develop methods and technologies to enable fully automated handling of biological samples under cryogenic working conditions. We focus on designing flexure hinges and monolithic gripper geometries and developing a wireless energy transfer system. The aim is to create the basis for the realisation of a robot-assisted handling system. For this purpose, optimal robot kinematics, suitable construction materials and electrical components had to be determined from the requirements of the targeted process. The components found and developed were then simulated, evaluated and compared in various program environments such as ANSYS. Based on these findings, we then design and test the above components to verify their functionality in cryogenic working environments.

In this paper, we first present related works, the basic concept of the robot structures, and the monolithic joints' design in sections 1.1 and 1.2. We then describe the experimental setup for verifying the functionality of the actual flexure hinges in section 2. We compare the data recorded in the experiments, such as the achieved bending angle, required bending moments, and maximum stresses that occur, with the values obtained in the simulations that we did in prior works to prove the functionality of the flexure hinges in section 3 and give an outlook on future research and developments in section 4.

1.1. Related work

In the past, there have already been many attempts to replace conventional rigid hinges and swivel joints with compliant mechanisms [3]. Flexure hinges and related monolithic joints are advantageous over common joints. They are almost impervious to soiling and abrasion, do not require lubrication and can readily be used in challenging environments [4,5]. Most works focus on small but very precise movements and components on a microscopic scale, employing relatively simple geometries for the hinges [6,7]. While this works for high precision and micro-movement applications, mechanisms that require larger displacements or bending angles significantly increase the complexity of the compliant mechanisms used. Flexure hinges for use in the extreme environments of aerospace applications have been presented in [8]. In addition, flexure hinges have been used in parallel robot structures by [9] and [10].

However, to the authors' knowledge, the use of complex flexure hinges as passive joints in a cryogenic work environment has not yet been investigated. By using complex monolithic flexure hinges, we can create joints able to withstand extreme temperatures while bearing occurring forces without any significant, unintentional deformations.

1.2. Basic structure and previous works

The parallel robot structure we develop is subject to several geometric constraints. One requirement of the project is that the entire drive technology must be located outside the cold area. We investigated parallel kinematic robot structures, in particular, both commercially available models and new structures. Based on previous works, we used evolutionary algorithms such as particle swarm optimisation and similar strategies to verify which designs best fit the intended application [11]. The optimisation parameters include (among others) the base and platform diameters, the length of the elements between the passive joints and the inclination of the conical base joints. The constraints limiting the designs include the geometric plausibility and self-collisions, the maximum installation space and maximum bending angles we anticipate for the flexure hinges [12]. We determined a delta structure with vertical drives in the form of electro spindles with Cardan joints as passive joint geometries as the most suitable.

Based on this selection, we designed several possible robot variants. For the design of the links and Cardan joints, we followed [9]. We aim for the continued improvement of the designs, primarily at reducing the number of components and the dead weight of the structure. Figure 1 (a) shows the current favoured structure. The Cardan joints themselves are composed of individual flexure hinges, as shown in figure 1 (b). These flexure hinges (shown in figure 1 (c)) are intended to realise the function of the Cardan Joints as univalent swivel joints. They are subject to extremely high requirements due to the unique environmental conditions of the cryogenic workspace.

We had to investigate a wide variety of boundary conditions and prerequisites for the use and design of flexure hinges in a cryogenic environment. We analysed how the material properties (Young's modulus, elongation, yield strength)

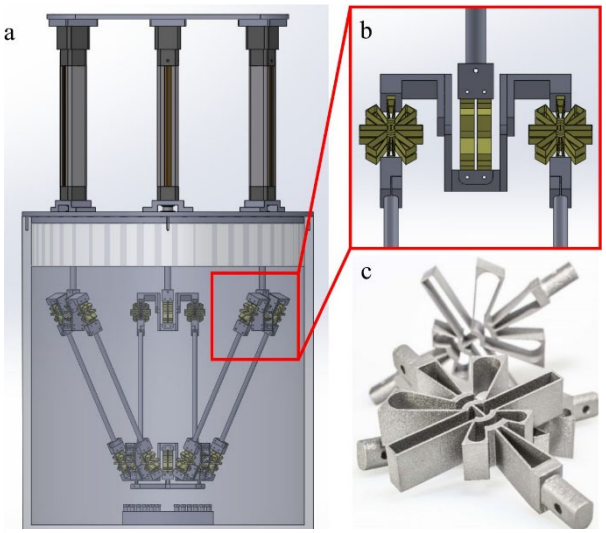

Fig. 1 (a) Structure of the parallel robot; (b) single Cardan joint with substituted flexure hinges; (c) actual flexure hinges

change under cryogenic ambient conditions and which permissible generally valid limits we could define. We paid particular attention to materials already used in refrigeration engineering, such as spring steels or Teflon-based polymers. In

order to validate the suitability of these materials, we designed and constructed flexure hinges according to the material-specific boundary conditions. We then modelled the flexure hinges using ANSYS FEM software, incorporating the target temperature levels below -130°C by adapting the values for Young's modulus and Poisson's ratio and simulated the deformation behaviour. The various joint geometries were parameterised for this purpose to be able to vary the determining parameters (for example, joint cross-section, lengths of the deformed areas, corner radii) as desired, and thus to be able to investigate a large number of geometric manifestations [5]. Following on from the work of [13,14], we identified a cascaded solid pivot joint as the most promising design candidate for further developments.

1.3 Simulations

The joint we chose in section 1.2 serially connects 16 regions of reduced cross-section. In addition to the desired rotational motion, we must consider force-deformation characteristics along the major and minor axes as well as dimensional stability. We identify the relevant load paths and highest stressed points of the design candidates. Then, we vary the material distribution within the allowable design and production conditions to generate all possible joint geometries for comparative study. Figure 2 shows an example of the initial geometry models (a) and a modified geometry (b).

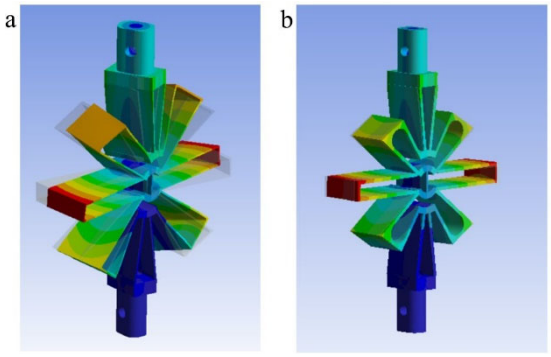

Fig. 2 (a) initial geometry model; (b) modified geometry

Figure 3 shows the geometric changes in more detail, with an unaltered hinge (a), the greater overall thickness of the bending points (b), shortened component elements (dubbed wings) (c), and reinforcements between the bending points (dubbed shuttles) (d). Finally, we evaluate the changes in different load cases. We take care to ensure that the maximum equivalent stresses encountered do not exceed the maximum stresses that the material can withstand under cryogenic conditions and that a bending angle of at least 30° is always achieved.

We presented the results for these analyses in previous works [15]. The adjustments to the geometric parameters have the primary goal of minimising the undesirable deformation of the flexure hinge along the parasitic axes without limiting the primary function of the rotational joint. In this context, parasitic axes are all spatial axes that are not the primary bending axis

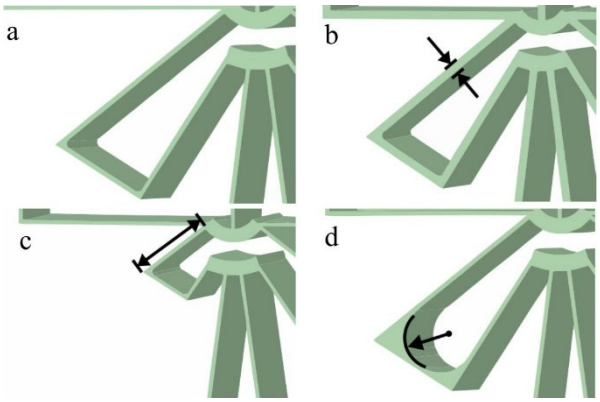

Fig. 3 (a) unaltered geometry; (b) increased material thickness; (c) shortened wings; (d) increased shuttle radius

of the flexure hinge. We were able to show that geometric adjustment of the flexure hinge geometries allows a significant reduction (up to 95%) in deviations from the optimal pivot point of the flexure hinges without limiting functionality or exceeding the critical equivalent stresses and strains. Table 1 shows the target parameters maximum strains, stresses, necessary bending forces and deviations from the optimal target position under different load cases for the unaltered flexure hinge (base design) and modified flexure hinges.

Table 1 The target parameters maximum strains, stresses, necessary bending forces and deviations from the optimal target position

Design Candidate	Bending Force [N]	Deviation from pivot point [mm]	Maximum strain at 30° [%]	Maximum stress at 30° [MPa]
094	54,716	0,338	0,603	754,83
178	143,84	0,144	0,763	953,755
048	29,716	0,576	0,562	653,158
096	57,48	0,311	0,637	796,996
137	93,444	0,207	0,694	868,236
222	218,49	0,092	0,865	1082,956
Base	17,241	1,609	0,303	378,97

Table 2 The geometric parameters for the design candidates and the initial design from [9] as a reference

Design candidate	Thickness of bending points [mm]	Wing shortening [mm]	Shuttles upper wing [mm]	Shuttles lower wing [mm]
094	0,2	10	1,6	2,4
178	0,4	10	1,3	2
048	0,2	10	1,6	3,2
096	0,1	10	1,6	3,2
137	0,3	10	1,6	2,4
222	0,5	10	1,0	2,8
Base	0,1	0	0	0

However, the results indicate no linear relationship between the target variables and the individual geometry parameters. We assume that the parameters themselves depend on each other in their effect on the target parameters, and no linear regression model can be used as a basis for optimisation. Therefore, we chose a multidimensional Pareto analysis as the optimisation strategy. The Pareto analysis allows us to evaluate and compare all the design candidates regarding the target criteria (bending forces, maximum stress and deviations from

the optimal position). Based on this optimisation strategy, we selected six design candidates for further analysis. Table 2 shows the geometric parameters for the design candidates together with the values for the initial flexure hinge from [14].

All candidates reduce the deformation along the parasitic axes significantly but deviate in their geometric properties (except for the shortened wings), predicted maximum stresses and necessary bending forces.

2. Setup

In this section, we will introduce the test rig for the developed flexure hinges, and we will explain the test setup in detail.

2.1 Hard- and software setup

To validate the characteristic target parameters obtained from the simulations, we built a test bench for bending tests in a cryostat from the company Cryotherm (CM2000). The test bench consists of a programmable logic controller (PLC, CX9020), a stepper motor with a reduction gear (AS2023), a motor terminal (EL7074) and a 4-channel measuring bridge (ELM3504-000) from Beckhoff. Figure 4 shows the test rig;

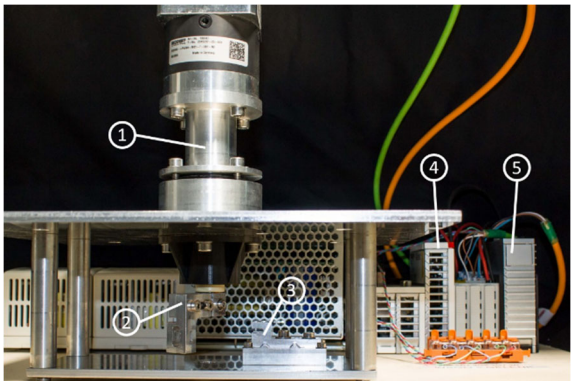

Fig. 4 complete test rig: (1) stepper motor, (2) lever arm, (3) clamping mechanism, (4) PCL and motor terminal, (5) measuring bridge

figure 5 shows a detailed view of the clamping mechanism. The logic controller enables us to operate the test rig and provides the necessary electric currents for the stepper motor and measuring bridge. The test rig has a TwinCAT 3 runtime, a visual development environment for configuration of control, drive control as well as in- and outputs. The components are connected with a BUS-System.

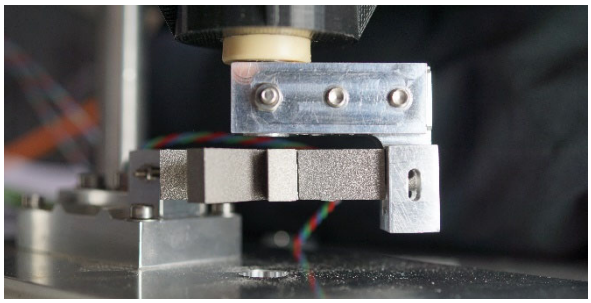

Fig. 5 detailed view of the clamping mechanism inside the test rig

The design of the test rig allows us to apply an exact bending angle to the flexure hinge. The placement of the motor shaft directly over the pivot point of the flexure hinge also allows a pure torque to be applied around this pivot point without inducing motion along other axes. The motor shaft (1) is directly over the pivot point of the flexure hinge; the torque is applied on the right side with a lever arm (2) while the flexure hinge is securely clamped to the base of the test rig (3). Using the stepper motor with a high reduction ratio, we can set angles with a resolution of 0.15°. The stepper motor itself also provides data to the logic controller (4) of the motor current required to move, so it is possible to calculate the holding torque for the set bending angles.

As described in section 1.2, the strains and stresses occurring in the components represent the characteristic value limiting the flexure hinges' achievable bending angles. To be able to calculate the strains, we fit each flexure hinge with two strain gauges. The strain gauges from Preusser (CFLA-1-350-11-6FA1LT-F) and the adhesive for fixing them to the flexure hinges are especially suited for use in cryogenic working environments. We fix the strain gauges on or near the areas on the flexure hinges that showed the highest stress values in the simulations. The strain gauges are connected in the 4-channel measuring bridge (5) to form a half-bridge in the three-wire circuit to increase the measurement system's sensitivity. This ensures that the cables connected to the strain gauges do not affect the resistance values in the circuit. The three-wire circuit compensates, among other things, for the resistance changes the cables experience due to temperature effects. The programmable logic controller also allows direct conversion of the voltage changes occurring in the strain gages into the corresponding strains that occur in the areas of the flexure hinge under investigation. If the strain gauges are installed correctly, the manufacturer guarantees a standard deviation of less than 1% for the measured values. The measuring bridge itself provides a maximum sampling rate of 100 µs with a measuring uncertainty of 0,05%.

2.2 Test objects

We manufacture the design candidates as functional samples for subsequent tests using the SLM process, as this manufacturing method allows extremely high accuracies even for tiny geometric details. Figure 1 (c) shows a selection of the finished flexure hinges. However, due to the manufacturing process itself, we are limited in our choice of the base material. We use the titanium alloy TiAL6V4. This alloy is one of the most common alloys for 3D metal printing and combines excellent mechanical properties with extremely low weight. This material has good corrosion resistance and is often used in demanding applications such as aerospace. In addition, the material's properties at cryogenic temperatures are well documented. The significant factor here is the yield strength of the material, which is about 1 % strain and maximum stress of 1250 MPa [16]. For the simulations described in section 1.3, we assume that only 90 % of these values are achievable upper limits for safety (0,9 % strain and maximum stress of 1125 MPa).

.

2.3 Experimental Setup

To evaluate the feasibility of the chosen flexure hinges, we perform three types of test scenarios with each of the selected joint geometries:

- Verification of the strains and stresses occurring at fixed bending angles.
- Fatigue tests over 10,000 test cycles for defined bending angles
- Bending until failure of the flexure hinge

We use the first test series to validate the data obtained in the simulations for maximum occurring strains and stresses and necessary bending moments. We will discuss the data obtained here in more detail in the following section. We bend the flexure hinges in three steps to an angle of 30° and hold there for 60 seconds for these tests. We then switch the motor moment-free to verify that the flexure hinge springs back to its original position on its own. In addition to recording the moment and strain values, this serves as an indicator of purely elastic deformation. The second and third series of tests demonstrates that the permanent use of the flexure hinges is possible over an extended period of time while maintaining a certain level of safety. In the permanent load test, we bend the flexure hinges 10,000 times to an angle of 30° and observe any changes in the motor current values and the resistance values of the strain gauges. We perform these bending tests until the flexure hinges fail by bending each one beyond the target angle of 30°, with an increasing bending angle in 5° increments. We then hold the flexure hinges in position for 5 minutes to record any changes in motor current and strain gauge resistance values. We continue this until the flexure hinges snap or break under load. Figure 6 shows the general approach. The data processing block does not affect the input parameter in subsequent test cycles. It converts the data into a further usable format and a first visual representation.

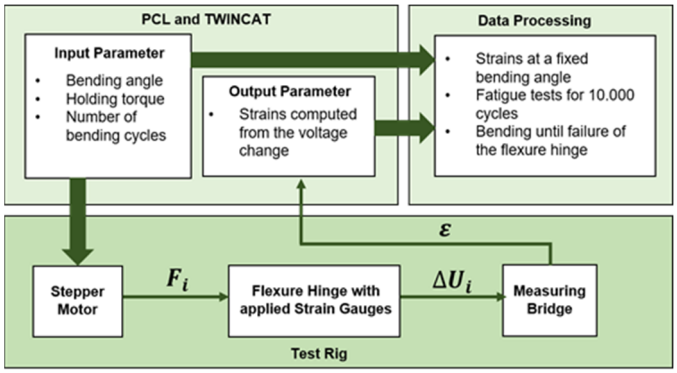

Fig. 6 visualised approach for the three tests cycles.

We can now compare the values recorded in this way with the characteristics obtained in the simulations to determine whether the simulations' behaviour correlates or even matches the actual properties.

3. Experimental results

After completing the test series, we determined that all selected joint geometries achieved the required bending angle of 30° without plastic deformation of the flexure hinges. All geometries endured both the single and the endurance tests without damage. Unfortunately, for two of the design candidates (137 and 178), the strain gauges failed during the tests due to broken cables. The values recorded during the tests for the maximum strains and stresses occurring in the areas investigated were lower than the values predicted in the simulations. Table 3 compares the simulated values of the strains and stresses and the absolute measured values for four of the design candidates from the bending tests.

Table 3 Comparison of simulated strains and stresses with the strains and stresses measured during the test cycles

Design candidate	Simulated maximum strains (%)	Measured maximum strains (%)	Simulated maximum stresses (*MPa*)	Measured maximum stresses (*MPa*)
048	0,56	0,52	701,01	653,15
094	0,60	0,55	754,83	695,0
096	0,63	0,61	796,99	727,5
222	0,86	0,82	1082,96	1034,0

One reason for the deviating values could be the occurring manufacturing errors. Figure 1 (c) shows that the surface areas are very grainy, and finer structures are deformed prior to applying any force. Another reason for the significantly higher strain and stress values in the simulations may be the meshing of ANSYS components. Due to the complex and often extreme geometries of the flexure hinges, tetrahedron-shaped mesh elements are often used in the meshing. However, this causes unrealistically high values for the stiffness of the simulated component. We try to counteract this behaviour by finer meshing (and thus increasing the number of mesh elements) of the features in the areas with the highest density of tetrahedron-shaped mesh elements. However, due to the vast number of simulations, we must compromise between the realistic behaviour of the mesh and a sufficiently short simulation time.

The fatigue tests' evaluation show no change in the recorded parameters (motor current and resistance values of the strain gages) during the test cycles considered. The flexure hinges all exhibit purely elastic behaviour and show no discernible deformation or damage during subsequent testing. The bending tests until failure of the flexure hinges yield two crucial results:

On the one hand, we are able to show that the flexure hinges exhibited the elastic behaviour demonstrated by the ANSYS simulation. Each of the flexure hinges investigated has - depending on the selected parameter configuration of joint cross-section, lengths of the deformed areas and corner radii - a unique maximum bending angle. This is the angle just before entering the area of plastic deformation (the selected limit here is 90% of the maximum strains and stresses). Each of the checked flexure hinges reaches this unique angle without reaching the threshold of 0,9% strain. The angles at which the

selected flexure hinges fail exceeds the expected angles, in some cases by almost double. Table 4 compares the simulated values for the unique bending angles with the actual angles, at which three of the design candidates fractured.
Comparison of simulated maximum bending angles from ANSYS simulations and actual bending angles measured during the tests until fracture

Table 4 Comparison of simulated maximum bending angles from ANSYS simulations and actual bending angles measured during the tests until fracture

Design candidate	Simulated maximum bending angle (°)	Measured maximum bending angle (°)
094	49	65
096	45	60
222	33	57

4. Summary and Outlook

In this paper, we were able to show that the flexure hinges we selected after simulation and optimisation can perform their intended task in the parallel robot structure. The values for maximum strains and maximum stresses obtained from the simulations were not exceeded by the hinges in the tests, neither in the individual tests nor in the endurance tests. The load tests at a bending angle of 30° correspond to the planned application case. Furthermore, we were able to show that the individual critical bending angles by the joints without plastic deformation were achieved by all tested joints and, in some cases, significantly exceeded. Thus, we can guarantee sufficient safety of the joints against failure, despite the described problems and errors in the production of the design candidates.

The simulations and experimental investigations presented in this paper focused primarily on the deformation of the flexure hinges about their axis of rotation. However, since flexure hinges are monolithic structures (i.e., made from a single piece), the deformations of these components are not limited to this one primary axis. Instead, under actual conditions, the entire joint is deformed along and about all three spatial axes. In [15], we have already investigated the deformation behaviour of flexure hinges about undesirable secondary axes (so-called parasitic axes) in ANSYS simulations. An experimental investigation of these deformations is still pending. In addition, we must expect that the flexure hinges are subjected to a superposition of different load cases in actual use in the parallel robot structure. This superposition of deformations along or around several axes is challenging to investigate experimentally and can better be studied in the completed demonstrator.

In addition, there is a need for further research in the area of manufacturing itself. One of the joint geometries investigated did not fracture during the tests to component failure at the location we expected with the most significant simulated stresses. However, it withstood the critical loads we expected before the failure. In addition, the fracture point did have flaws in material inclusions that could have promoted the fracture. The highly intricate structures are very susceptible to such defects. Future developments in the design of flexure hinges must therefore include the limitations due to the manufacturing process even more in the considerations.

Acknowledgements

The authors acknowledge the support by the Deutsche Forschungsgemeinschaft under project number 349906175 (cryogenic handling)

References

[1] Anifandis, G., Messini, C. I., Simopoulou, M., Sveronis, G., Garas, A., Daponte, A., & Messinis, I. E. (2021). SARS-CoV-2 vs. human gametes, embryos and cryopreservation. In Systems Biology in Reproductive Medicine, pp. 1-10.
[2] Lermen, D., Bloemeke, B., Browne, R., Clarke, A. N. N., Dyce, P. W., Fixemer, T., ... & Mueller, P. (2009). Cryobanking of viable biomaterials: implementation of new strategies for conservation purposes. In Molecular Ecology, 18(6), pp. 1030-1033.
[3] Linß, S., Schorr, P., Zentner, L. (2017). General design equations for the rotational stiffness, maximal angular deflection and rotational precision of various notch flexure hinges. In Mechanical Sciences. pp. 29-49.
[4] Kern, D., Rösner, M., Bauma, E., Seemann, W., Lammering, R., Schuster, T. (2013). Key features of flexure hinges used as rotational joints. In Forschung im Ingenieurwesen, 77(3-4), pp. 117-125.
[5] Dirksen, F. (2013) Non-intuitive design of compliant mechanisms possessing optimized flexure hinges (dissertation). pp. 12-13
[6] Cannon, J. (2004) Compliant Mechanisms to Perform Bearing and Spring Function in High Precision Applications (dissertation). p.15
[7] Lates, D, Noveanu, S. Csibi, V. (2014) Micropositioning system with flexure hinges for microfactories. In: Key Engineering Materials. Trans Tech Publications Ltd. pp. 485-490.
[8] Zirbel, S. (2014) Compliant Mechanisms for Deployable Space Systems. Brigham Young University (dissertation).
[9] Hesselbach, J., & Raatz, A. (2000). Pseudoelastic flexure hinges in robots for microassembly. In Microrobotics and Microassembly Vol. 4194, pp. 157-167.
[10] Kozuka, H., Arata, J., Okuda, K., Onaga, A., Ohno, M., Sano, A., Fujimoto, H. (2012). A bio-inspired compliant parallel mechanism for high-precision robots. In 2012 IEEE International Conference on Robotics and Automation pp. 3122-3127.
[11] Schappler, M., Ortmayer, T. (2020), Dimensional synthesis of parallel robots: Unified kinematics and dynamics using full kinematic constraints, In 6. IFToMM D-A-C-H Conference.
[12] Schappler, M, Jahn, P, Raatz, A, Ortmaier, T. (2021) Combined Structural and Dimensional Synthesis of a Parallel Robot for Cryogenic Handling Tasks, In Annals of Scientific Society for Assembly, Handling and Industrial Robotics (accepted)
[13] Fowler, R. M. (2012). Investigation of compliant space mechanisms with application to the design of a large-displacement monolithic compliant rotational hinge.
[14] Fowler, R. M., Maselli, A., Pluimers, P., Magleby, S. P., Howell, L. L. (2014). Flex-16: A large-displacement monolithic compliant rotational hinge. Mechanism and Machine Theory, 82, pp. 203-217.
[15] Jahn, P., Raatz, A. (2020): Numerical simulation and statistical analysis of a cascaded flexure hinge for use in a cryogenic working environment, In: Annals of Scientific Society for Assembly, Handling and Industrial Robotics. pp 81-94.
[16] ASM International 2002: Atlas of stress-strain curves: ASM International. Materials Park, Ohio. 2. Ed, p. 222